Light-addressable electrochemistry at semiconductor electrodes: redox imaging, mask-free lithography and spatially resolved chemical and biological sensing

Equation Chapter 1 Section 1
Received 00th January 20xx,
Accepted 00th January 20xx

DOI: 10.1039/x0xx00000x

www.rsc.org/

Yan B. Vogel,[a] J. Justin Gooding *[b] and Simone Ciampi *[a]

Spatial confinement of electrochemical reactions at solid/liquid interfaces is a mature area of research, and a central theme from cell biology to analytical chemistry. Monitoring or manipulating the kinetics of a charge transfer reaction in 2D is generally achieved using scanning electrochemical microscopy or multielectrode arrays; techniques that rely on moving physical probes, or on a network of electrical connections. This tutorial is introducing concepts and instruments to confine faradaic electrochemical reactions in 2D, without resorting to the mechanical movement of a probe, and with the simple design of one semiconducting electrode, one electrical lead and a single-channel potentiostat. We provide a theoretical background of semiconductor electrochemistry, and describe the use of localised visible light stimuli on photoconductor/liquid and semiconductor/liquid interfaces to address electrical conductivity – hence chemical reactivity – only at one specific site defined by the experimentalist. This enables to shift the tenet of one electrode/one wire, toward one wire/many electrodes. We discuss the applications of this emerging platform in the context of surface chemistry patterning, redox imaging, chemical and biological sensing, generating chemical gradients, electrocatalysis, nanotechnology and cell biology.

Key learning points

(1) Theoretical and historical background of semiconductor photoelectrochemistry.
(2) Spatial confinement of electrochemical reactions: advantages of using light over traditional methods (scanning probes techniques and multielectrode arrays).
(3) Applications of the light-addressable electrochemistry concept in:
- Mask-free micropatterning of metals, metal oxides, polymers and molecules on semiconductor and photoconductor surfaces;
- Chemical analysis by amperometric detection of adsorbed or diffusive analytes;
- Electrochemical microscopy;
- Generation of chemical gradients;
- Cell biology.
(4) Practical aspects of a light-addressable electrochemistry experiment: choice of photoelectrode material, experimental parameters and experimental designs, such as light pointer vs micromirrors or microprojectors, backside vs frontside illumination (at a dry interface vs across an electrolyte).

1. Introduction

Confining electrochemical reactivity only to a discrete area within the surface of a macroscopic electrode is important for a host of applications, from imaging catalytic surfaces to interrogating an array of sensing elements. Traditionally, restricting electrochemical events only to a specific site within the surface of a device has required a network of discrete metallic elements – an array of conductive pads electrically insulated one from another, and each individually linked to a multichannel potentiostat (Fig. 1a).[1] Arrays of electrodes have grown in popularity thanks to continuous advances in microfabrication techniques,[1] but they have shortcomings: a considerable amount of space on the chip's surface is used to house bonding pads, connections and insulating material; the position of each redox element in the array is fixed and pre-determined; and the 2D arrangement of redox active features of the sample may be a complete mismatch of the 2D arrangement of electrodes in the array, potentially impairing spatial resolution in reading voltages or delivering currents.

Strategies to obtain electrochemical 2D information (i.e. 'electrochemical reading'), or to guide locally redox reactivity (i.e. 'electrochemical writing'), based on scanning the surface of interest with micro-/nano-scopic electrodes – scanning probes techniques[2] – have removed the requirement of a network of conductive pads and electrical connections. Scanning electrochemical probe microscopy (SEPM, Fig. 1b), and in particular scanning electrochemical microscopy (SECM), are routinely employed in research that ranges from energy conversion to cell biology.[2] For instance, SEPM techniques can now claim spatial resolution of only few nanometres, and under particular circumstances, imaging speeds as high as few milliseconds per pixel. SECM has become a widespread laboratory tool, but it has the intrinsic characteristics of a scanning probe method: moving parts with possible disturbance of the system (e.g. hydrodynamic forces); the need for the

[a] *Department of Chemistry, Curtin Institute of Functional Molecules and Interfaces, Curtin University, Bentley, Western Australia 6102, Australia. Email: simone.ciampi@curtin.edu.au*
[b] *School of Chemistry, The Australian Centre for NanoMedicine and the Centre of Excellence in Convergent Bio-Nano Science and Technology, The University of New South Wales, Sydney, New South Wales 2052, Australia. Email: justin.gooding@unsw.edu.au*

Glossary

Semiconductor photoelectrochemistry: the study of chemical processes that are coupled to the flow of electricity at a semiconductor/liquid interface under electromagnetic (generally visible) radiation.

Light-addressable electrochemistry: localised (2D) changes to the thermodynamics and/or kinetics of an electrochemical reaction. The geometrical characteristics of the 2D pattern are specified on an unstructured semiconductor electrode by a light stimulus.

Photoeffects at semiconductors: the generation and recombination of free charge carriers in a semiconductor exposed to supra band gap radiation, and their movement under the influence of an electric field or a concentration gradient.

Photoelectrochemical microscopy: techniques to image the magnitude and dynamics of localised charge transfer heterogeneous reactions.

Photoelectrode: electrode capable of assisting electrochemical reactions when illuminated.

Photoanode/photocathode: photoelectrode giving an anodic/cathodic photocurrent, whose open circuit potential tends to shift cathodic or anodic (respectively) of the dark value upon illumination.

probe to raster the sample sequentially, line by line; and it provides only indirect information on currents and voltages. The last constraint – indirect redox information – arises because the probe has to approach the electrode from the electrolyte side, that is, in a SECM experiment the entire interface under analysis is generally biased and a steady-state current is recoded by an ultramicroelectrode giving an electrolyte "point of view" of the electrified interface. This implies that experimental *x*–*y* currents need correction to account for factors such as sample topography and tip geometry.[2]

Contact-less methods have emerged to remove some of these restrictions, which can be summarised as: poor use of space on a chip, fixed geometry of an electrode array, risk of a probe disturbing the system under analysis, and complex data analysis. Among these contact-less methods, of special relevance is the work done by Tao et al,[3] who developed an imaging technique to measure local electrochemical current densities as a function of optical signals (surface plasmon). This technique does not require scanning probes and is contactless, but on the other hand it does not allow the operator to manipulate local currents and voltages. Light-addressable potentiometric sensor (LAPS)[4] have analogous merits and shortcomings. A LAPS device consists of an unstructured semiconductor/insulator/liquid interface and uses an AC photocurrent, generated in response to a modulated light, to detect local changes in capacitance at the site of the illumination. LAPS however, analogously to plasmon-based methods, remain chemical sensors: with no net DC currents crossing the interface they cannot guide the electrochemical reactivity of the interface.

In this tutorial we review the concepts and recent applications of faradaic photoelectrochemistry for the spatial confinement of redox reactions on unstructured semiconductor electrodes; a concept referred here as light-addressable electrochemistry (Fig. 1c).[5] The influence of light on the electrical conductivity and electrochemical reactivity of semiconductors has been extensively explored in photovoltaics and photocatalysis.[6] In such experiments, a semiconductor biased into depletion behaves as an insulator, but is transiently turned into a conductor when illuminated with supra band gap light. A direct conceptual implication is the possibility of spatially localising in 2D a heterogeneous electrochemical event by confining in space the illumination stimulus. This removes the requirement for scanning probes, structured surfaces, or connecting pads. This approach, known as light-addressable electrochemistry (see Glossary), was demonstrated in the 1970s–80s for surface patterning[7] and photoelectrochemical imaging,[8] but its

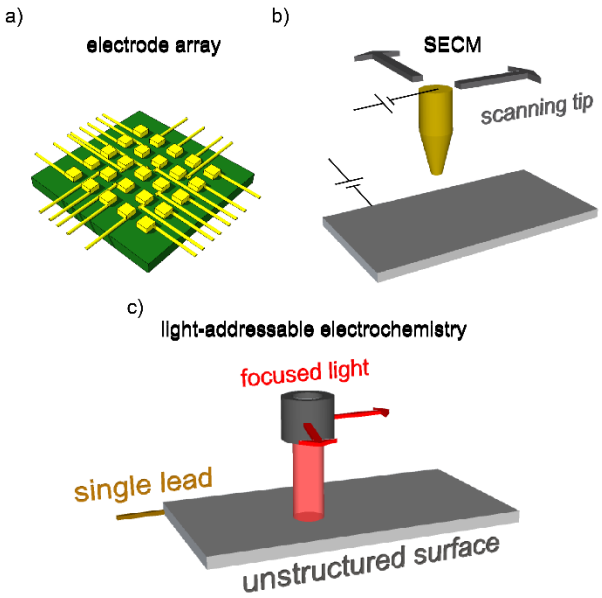

Fig. 1. Traditional and emerging concepts and tools to spatially confine electrochemical reactions in 2D. (a) Schematic depiction of an individually addressable multielectrode array (electrodes in yellow) secured on an insulating substrate (green in figure). Their operation requires a multichannel instrument. (b) Diagram of a scanning electrochemical probe microscopy experiment, showing the movement of an ultramicroelectrode to record a steady-state current as a function of its precise position over a biased (using a bi-potentiostat), or zero-bias, conductive or insulating substrate. (c) Light-addressable electrochemistry of an unstructured semiconductor or photoconductor. The electrode is biased into depletion, creating a near-surface barrier to charge transfer. A specific area of the surface is irradiated with a focused visible light beam and actuates a "conductive channel" to allow the flow of photogenerated charge carriers from the interface to a single peripheral electrical lead via the bulk electrode.

applications in chemical analysis,[5] cell biology,[9] lithography[10] and electronics[11] have only been made possible after recent developments in (i) surface chemistry to electrically stabilise non-oxide semiconductor surfaces under ambient, oxygen-rich conditions, and in (ii) optical instruments, such as digital micromirrors and spatial light modulators, originally used for super-resolution microscopy, to allow for greater freedom, speed, and accuracy in delivering the illumination stimulus.[12] Moreover, recently reports on the use of non-silicon photoelectrodes for light-addressable electrochemistry, such as hematite[13] and quantum dots,[14] are promising to push research in the field rapidly forward.

The structure of the review is as follows: in Section 2 we discuss the basis of photoeffects on charge-transfer reactions at semiconductors; in Section 3 we describe the concept of light-addressable electrochemistry with resolution on space and time; in Section 4 we review materials that have been used, or have the potential of being used, as photoelectrodes for light-addressable electrochemistry; in Section 5 we discuss advances in light-addressable electrodeposition ("electrochemical writing"); and Section 6 and 7 focus on "electrochemical reading". Section 6 describes on the use of light-activated conductive channels in the context of chemical sensing, and Section 7 outlines applications in redox microscopy. Section 8 introduces the light-addressed generation of chemical gradients. Finally, Section 9 gives an outlook of the field, highlighting challenges and future directions.

2. Photoeffects and photoelectrochemical reactions at semiconductors

2.1 Energetics of the semiconductor/electrolyte interface

Photoeffects at the semiconductor/electrolyte interface – the generation and recombination of charge carriers and their movements under the influence of an electric field – have been thoroughly studied since the 1950s. This area of electrochemical research became highly popular after the 1973 oil crisis, and led to for example to the discovery of water splitting by visible light at a TiO_2 photoanode.[15] What followed was a systematic study of photoeffects in semiconductor electrochemistry, resulting in applications in chemical analysis and energy production.[4, 14]

Energy diagrams, as those generally used in solid state physics, are fundamental to the understanding of photoeffects and photoelectrochemical reactivity of semiconductor/liquid interfaces. The convention is to draw energy-levels diagrams such that the energy of the system is lowered as electrons fall down toward the source of positive potential (i.e. drawn at the bottom of the diagram). Such diagrams are depicted in Figure 2a–c and explained briefly below (for more detailed information the reader is referred to the bibliography).[6] In a semiconductor the highest unoccupied and the lowest occupied energy levels, the conduction band (E_C) and valence band (E_V) edges, respectively, are separated by an energy gap (E_G). An important parameter describing the electrochemistry of a semiconductor is its Fermi Level (E_F), the energy at which the probability of electron occupation is 50% and a measure of the average electrochemical potential of the electrons in the solid. E_F is positioned between E_V and E_C, with its exact position depending on the doping level and type. For an intrinsic semiconductor it lies exactly in the middle of the gap, for an n-type semiconductor is positioned closer to E_C, and for p-type it is closer to E_V.

When a semiconductor is brought into contact with a liquid containing a single redox couple, equilibrium is reached by means of electrons crossing the interface until the energy levels from both phases align. That is, the semiconductor E_F and the liquid redox potential E_{redox} reach equal values (Figure 2a, here E_{redox} indicates the reversible potential of a single redox couple when the anodic current is equal to the cathodic current, thus equalling to the formal potential $E^{0'}$). As a consequence of this exchange of charges, a potential difference is established at the interface, which is distributed between the semiconductor space charge layer (SCL), and the electrolyte. The exponentially decaying ~~field~~ electrostatic potential of the SCL extends inside the semiconductor for about 10–1000 nm (as the carrier concentration increases, the thickness of the SCL region decreases), while the double layer is much narrower, usually few Å, depending on the electrolyte concentration. The amount of voltage drop in the SCL is given by the difference between E_{redox} and the so-called flat band potential, E_{fb}, which is the applied potential where there is no voltage drop in the SCL. Any electron (and hole) in the SCL will interact with this field, hence the energy bands are disturbed by this field. The bands will bend upwards or downward depending the sign of the immobile ionized dopants atoms or presence of an external polarization (accumulation and depletion of minority charge carrier depicted in Figure 2b and 2c, respectively). When in depletion, the SCL is of high resistance (and low capacitance) and charge transfer across the interface is impeded. E_{redox} is chosen so that it lies below E_C to block oxidation reactions in the dark for an n-type semiconductor (or reduction reactions for a p-type semiconductor). For a redox couple of E_{redox} above E_C the semiconductor acts like a metallic electrode. The essence of conductivity in a solid is that there must be a partially vacant energy band for electrons to accelerate under an electric field, therefore shining light of energy higher than E_G will excite electrons into the upper band, where they have plenty of unoccupied energy states into which they can move (Figure 2c). Photogenerated minority carriers – such as holes in an illuminated n-type semiconductor – accumulate creating an electrical field that opposes the SCL with the result of flattening the bands (the degree of flattening depends on the intensity of the light). For an n-type semiconductor, holes move up the valence band, towards the interface, and here act as a sink of electrons for electroactive species present on the solution-side of the interface (Figure 2c), while electrons are driven into the semiconductor bulk. The photooxidation occurs at a less positive potential than the required at a metallic electrode because the energy provided by the light shifts the electrode potential to more positive potentials and help drive the redox

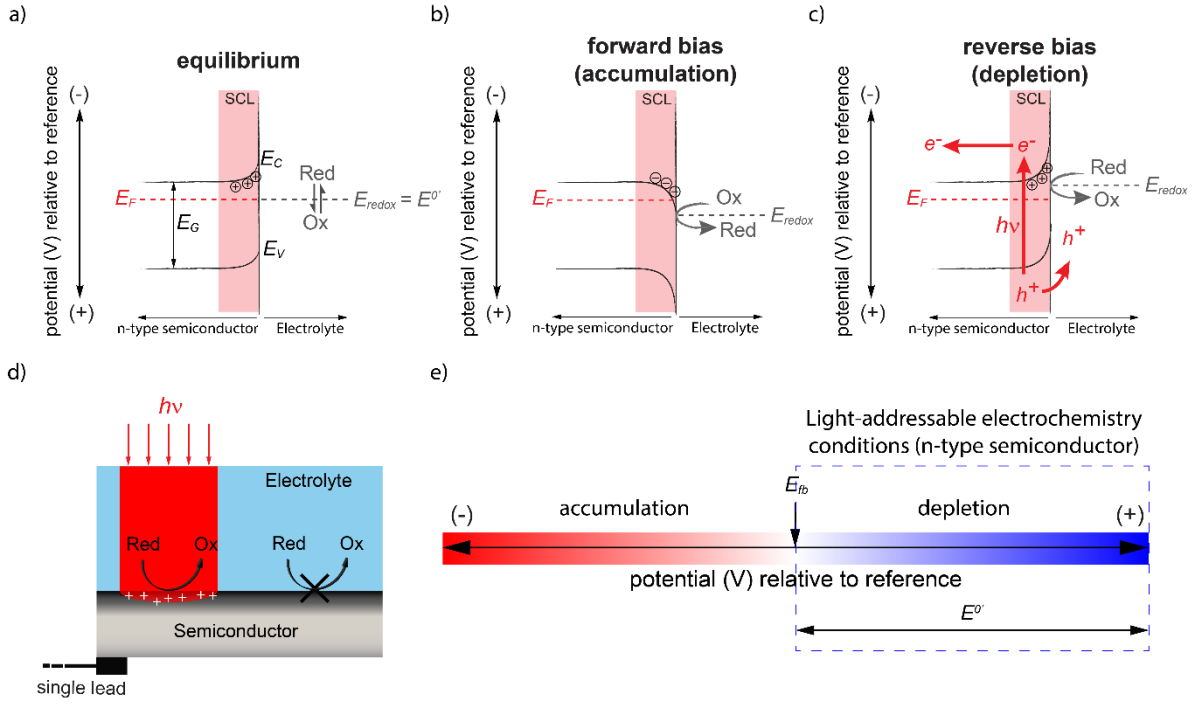

Fig. 2. Confining electrochemical reactions in 2D using light. The formation of a near-surface (10–1000 nm) space charge layer (SCL), together with the presence of an energy band gap, is at the origin of the photoelectrochemical properties of semiconductors. Band diagrams under (a) equilibrium, (b) forward bias and (c) reverse bias for an n-type semiconductor/liquid electrolyte interface. As an obvious consequence of the initial disparity between the concentration of electron and holes, electrode illumination will result in negligible changes in the concentration of majority charge carriers, but will induce a significant increase in the concentration of minority carriers. Photoeffects will therefore be more pronounced in depleted electrodes, that is, when light-generated minority carriers will migrate toward the electrode surface and dominate charge transfer and charge transport. The photoexcited electrons move into the bulk of the semiconductor, while a flux of holes migrate to the interface. A hole-mediated oxidation of a soluble electron donor is shown in (c). In an n-type electrode the bands are bent upward and are assumed to be pinned at the silicon-monolayer interface. (d) Illustration of the principle by which a faradaic process is light-assisted at a semiconductor electrode in the presence a SCL. Here the depleted SCL is used to spatially confine an electro-oxidation reaction by removing a surface kinetic barrier only at the illumination site. (e) Bias regime required to perform light-addressable electrochemistry (photooxidations) on an n-type semiconductor. Photoeffects would dominate charge transfer in a p-type material that is biased cathodic of its flat band potential (E_{fb}).

process. The amount of this contra-thermodynamic shift is given by the open circuit photovoltage E_{OC}:

$$E_{OC} = \frac{BRT}{nF} \ln\left(\frac{I_0}{I_L + I_0}\right)$$

where I_L and I_0 are the photogenerated and reverse diode current, respectively, B is the diode quality factor, while R, T, n and F have their usual meaning.

In practice however E_{OC} (max) often sits below this theoretical value due to kinetic processes (such as carrier recombination or electron transfer) occurring at the semiconductor/electrolyte interface, affecting photovoltages and photocurrents.

2.2 Flat band potential determination

Considering the above discussion on ensuring that a semiconductor electrode is in depletion to benefit from photoeffects, it becomes obviously important to first estimate E_{fb}: the potential where we move between depletion and accumulation (Figure 2e). One of the most common methods of estimating E_{fb} is that of measuring the SCL capacitance, C_{SCL}, as a function of the electrode bias. In a depleted electrode C_{SCL} is the smallest capacitance of a series arrangement and therefore dominates the total capacitance of the system. According to the Mott-Schottky equation:

$$1/C_{SCL}^2 = \frac{2}{A^2 N_D q \varepsilon}\left[\left(E - E_{fb}\right) - \frac{k_b T}{q}\right]$$

by plotting $1/C^2_{SCL}$ vs the applied potential, E, one should obtain a straight line in the bias window that corresponds to the electrode depletion. Here A is the electrode area, ε is the dielectric constant, q is the elementary charge and k_b is the Boltzmann constant. The intersection of the line with the potential axis gives E_{fb} + 26 mV, and the slope of the line has information on doping level N_D and can be used as a diagnostic test to check the quality of the measurement. The capacitance measurement is performed under dark conditions, and usually by an electrochemical impedance experiment done at different AC frequencies. Impedance measurements are extremely sensitive to electrochemical non-idealities and surface conditions, and therefore frequency dispersion in C_{SCL} is commonly encountered in such experiments. Other common

methods to estimate E_{fb} involve measurements of open-circuit voltages at large illumination intensities, or measurements of the onset of a photocurrent in a linear sweep voltammogram.

Once E_{fb} is known, the system can be biased into depletion, i.e. the potential window where under the SCL is of high resistance and low capacitance and where photoeffects are maximised. As discussed above, this regime is anodic of E_{fb} for n-type photoanodes and cathodic of E_{fb} for photocathodes. This is a requirement, but not a condition sufficient to perform light-addressable electrochemistry. It is also necessary to ensure the formal potential ($E^{0'}$) of the redox couple of which we are trying to alter oxidation or reduction rates to be located inside the depletion regime (Figure 2e). If $E^{0'}$ falls in the accumulation regime the electron transfer will occur even under dark conditions. Caution has also to be taken not to enter in the inversion regime, where an applied reverse bias sufficiently beyond E_{fb} will tilt E_v at the interface to the point of crossing E_F and therefore electron transfer will happen even in the absence of light. However, as we will see in Section 4.1, these requirements on the relative position of $E^{0'}$ and E_{fb} and are not a strict requirement for light-activated electrochemistry performed using thin layers of intrinsic semiconductors with fast recombination rates.

2.3 Electron transfer kinetics at the semiconductor/liquid interface

So far we have focused on the energetics of semiconductor/electrolyte interfaces without paying much attention to the kinetics of the faradaic reaction at the electrode surface. Light-addressable electrochemistry guides reactions in 2D such that they become locally both energetically as well as kinetically favourable. A sound understanding of the kinetics of the light-assisted charge transfer processes is therefore fundamental. Kinetic aspects can be divided into two categories, recombination kinetics and electron transfer kinetics. Recombination is the process where photogenerated minority carriers annihilate when they recombine by falling back into 'empty' states. Recombination kinetics is intimately related to carrier diffusion lengths and carrier lifetimes, and these will be discussed in the next section. For now we focus on the electron transfer kinetics which requires a short digression on metallic electrodes. The rate for a heterogeneous redox process occurring at a metal electrode is controlled by changing the potential difference across the double layer (a metal cannot hold a potential difference). Applying to a semiconductor a voltage against a suitable reference results in this potential distributing between the SCL and the double layer (Fig. 3a). Hence, changes to the photocurrent are brought about by changing both the electron/hole concentration at the semiconductor surface (by either changes on the applied potential or on the light intensity) and the electron transfer rate constant k_{et} (by the applied potential).[16]

Therefore, the exact form of a current–potential trace depends on the electron transfer kinetics, mass transport and, under illumination, on the flux of photogenerated charge carriers.

The treatment of the electron transfer kinetics at semiconductor electrodes has been pioneered by Gerischer and Lewis.[17] The dark current–potential relationship is given by the second order rate law:

$$J(E) = -qk_{et}[A]n_s$$

where $J(E)$ is the current density, q the elementary charge, $[A]$ the concentration of the acceptor species in solution and n_s the electron concentration at the interface, given by:

$$n_s = N_d e^{q(E_{fb}-E)/(k_B T)}$$

where N_d is the doping concentration and k_B the Boltzmann constant.

The value of k_{et} can be therefore obtained from steady state current–potential curves for semiconductor electrodes, as opposite to dynamic techniques usually needed for metal electrodes. This treatment is valid for a system when the charge transfer occurs from the conduction band (i.e. under dark conditions), is not limited by mass transport, and most of the potential drops in the SCL, and E_C and E_V are far from E_{redox}. It is worth noting that in this model the concentration of electric carriers, in cm^{-3}, is not included in the expression of k_{et}, and therefore the units of k_{et} are cm^4s^{-1}. Moreover, applying a potential affects the current density not by changing k_{et} but by changing n_s. Also, k_{et} is independent of E and dependent on E_C and E_{redox}.

Under illumination the charge transfer occurs via photogenerated minority carriers from the valence band. An accurate description of the electron transfer requires the use of a model that describes accurately the potential distribution at the semiconductor interface. The current–potential expression can be obtained by considering the series arrangement of E_{SC} and E_{DL} (see Fig. 3a), each having its characteristic current–potential response. As a consequence, k_{et} needs to be retrieved with a dynamic technique that allows to separate these two contributions, such as cyclic voltammetry.[16, 18]

We recently described an analytical model that allows to retrieve kinetic rate constants from cyclic voltammetry curves of redox monolayers attached on semiconductor electrodes under illumination.[16, 18] In this model, the SCL contribution to the current (I_{SC}) is given by the diode equation:

$$I_{SC} = I_{ph} + I_0\left[1 - \exp\left(-\frac{nFE_{SC}}{BRT}\right)\right]$$

where I_{ph} is the photogenerated current, I_0 is the reverse diode current, B is the diode quality factor and n, F, R and T have their usual meaning.

The double layer contribution is given by the Laviron equation, and SCL effects can be grouped into a single parameter θ :

$$\theta = \frac{I_{p,rev}}{|I_{ph}| + I_0}$$

where $I_{p,rev}$ is the peak current under Nernstian conditions.

The parameter θ depends on the scan rate and on G through $I_{p,rev}$ as well as on the light intensity through I_{ph}. G is a parametric measure of the overall interactions sensed by the redox

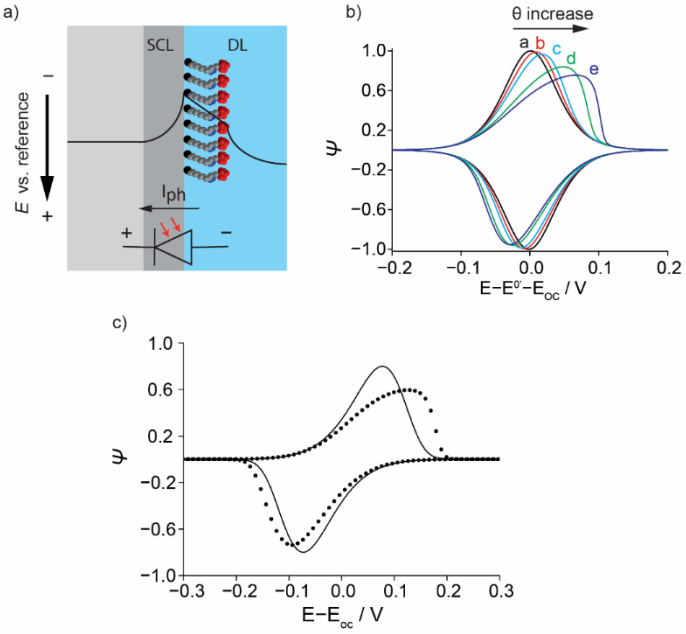

Fig. 3. Cyclic voltammetry model for obtaining electron transfer kinetics for a photoelectrochemical reaction at a photoanode. (a) Representation of the potential drop across the space charge layer (SCL) and double layer (DL). In the model, the potential drop across the SCL is considered as an ideal diode. (b) Shape of the voltammetric curves as a function of the parameter θ (see text), assuming completely reversible electron transfer kinetics and neglecting intermolecular interactions. From curve **a** to curve **e**, θ increases from $7.8{\cdot}10^{-3}$, $7.8{\cdot}10^{-2}$, 0.156, 0.389 to 0.519. (c) Simulated cyclic voltammetry for a metallic electrode (solid line) and for a n-type semiconductor electrode in the presence of diode effects (symbols, the value of θ is set to 0.7). Sweep rate is 0.1 Vs^{-1}, G = 0, α = 0.5 and $k_{et,ap}$ =1 s^{-1}. $\psi = \frac{I}{I_{p,rev}}$, with $H = \frac{RT}{n^2 FvQ}$, and $I_{p,rev}$ given by $I_{p,rev} = \pm\frac{1}{H}\frac{1}{4-2G}$, and where v is the potential sweep rate, Q is the total electrical charge transferred and R, T, n and F have their usual meaning. G is a parameter accounting for the overall interactions (attractive and repulsive) experienced by the redox centre. Adapted from ref. [16] with permission from Elsevier, copyright 2019.

monolayer: $G > 0$ corresponds to net attractive interactions (e.g. long-range electrostatics, or short-range π–π or van der Waals), $G < 0$ to net repulsive interactions (mainly electrostatics), and $G = 0$ corresponds to a situation of no interactions or where attractive and repulsive interactions cancel each other out.[19] An example of the effect of changes in θ on a simulated cyclic voltammogram is shown in Fig. 3b for an infinitely fast charge transfer kinetics and $G = 0$. The peak-to-peak separation, which in a metal electrode is an indication of k_{et}, increases with θ and it is solely due to the SCL contribution to the potential drop because in these simulations kinetics is infinite. As a consequence, the charge transfer kinetics cannot be retrieved in a straightforward manner from the peak-to-peak separation, for example using the Laviron model for a metal electrode. To reinforce on this point, Fig. 3c compares voltammograms simulated using either the "metallic" Laviron model (solid line) or the "semiconductor model" (symbols) under the same kinetics.

It is therefore obvious that analysing voltammetry data of a semiconductor electrode needs to be performed using a semiconductor model, where the SCL potential drop is considered, otherwise k_{et} could be largely underestimated.[16] The procedure to retrieve k_{et} is as follow: at strong illumination and low scan rates the full width at half maximum is independent on θ and only depends on G, which is then obtained. At slow scan rates, the peak separation is independent on k_{et} (reversible limit) and θ can be obtained by analysing data recorded at different light intensities. Finally, once θ and G are known, k_{et} is obtained through a scan rate study at high light intensity.

3. 2D confinement of photoelectrochemical reactions

Section 2 has covered the fundamentals of photoconductivity and photoelectrochemistry: mature areas of research in which light is used to generate electrical carriers and drive electrochemical reactions. Section 3 focuses on the fundamentals for the 2D confinement of photoelectrochemical reactions at an electrified semiconductor/liquid interface, which we refer as light-addressable electrochemistry.

3.1 Carrier recombination

For an electrochemical reaction to be confined to a well-defined or as small as possible region, the diffusion of the photogenerated minority carriers away from the illumination site and into adjacent dark areas needs to be minimised. A wealth of practical and fundamental knowledge when dealing with the confinement of photogenerated minority carriers in 2D can be gained from the field of light-addressable potentiometric sensors (LAPS).[4] Research in LAPS has shown that minority carriers may be found several micrometres away from the illuminated area because of their lateral diffusion, hence seriously affecting the 2D spatial resolution of the surface potential measurement (Fig. 4a).[4] The diffusion length, L, defined as the average length a carrier moves between

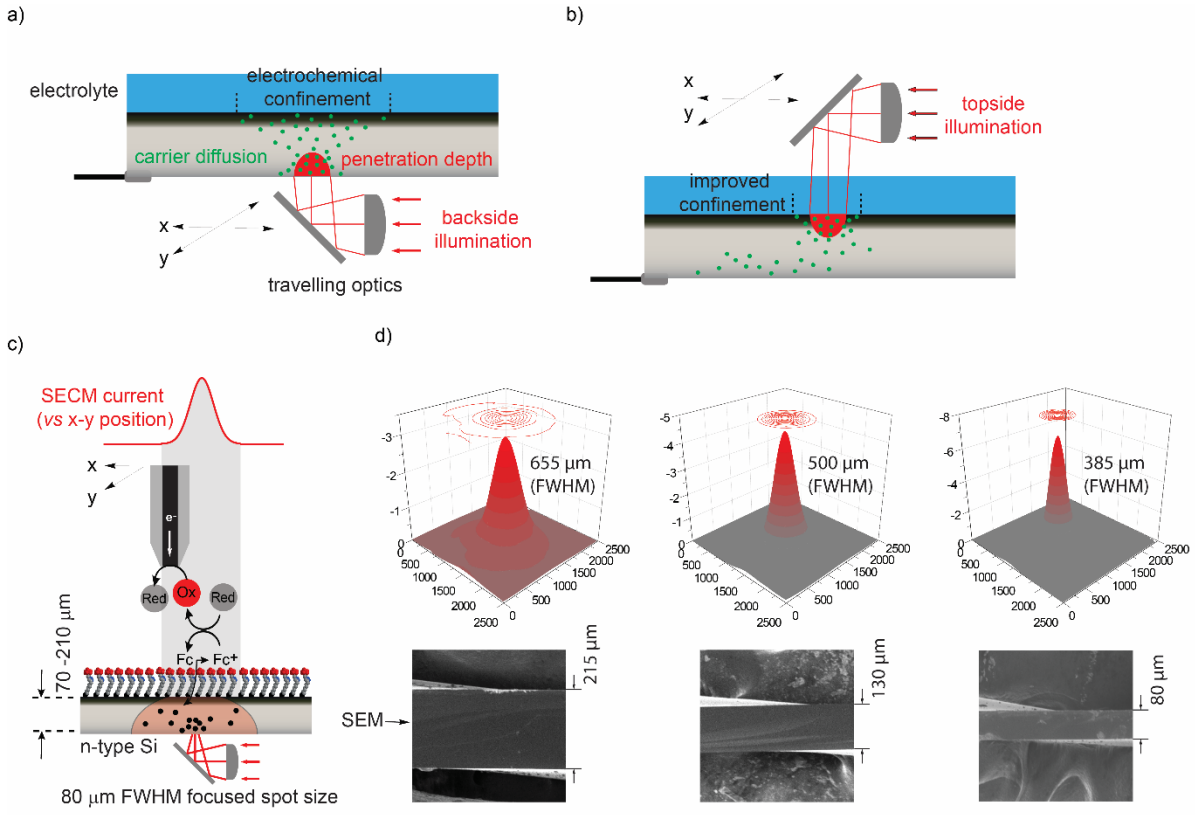

Fig. 4. Spatial confinement of photoelectrochemical reactions. Carrier diffusion in a backside (a) or in a top-side (b) illumination experiment. (c) The light-addressability of a model heterogeneous electro-catalytic reaction is mapped using a substrate-generation/tip-collection SECM apparatus. The faradaic process (Ox/Red) is light-assisted at a ferrocene-modified silicon electrode. At this photoanode, the oxidizing power of the generated ferricenium is sufficient for the oxidation of solution $[Fe(CN)_6]^{4-}$ to $[Fe(CN)_6]^{3-}$. Redox reactivity is confined to a discrete site on the electrode surface as defined by the position of a back-side light pointer. (b–d) The diffusible product of the heterogeneous electrode reaction (Ox = $[Fe(CN)_6]^{3-}$) is collected by a platinum UME to generate a two-dimensional map across the macroscopic electrode of the redox process. This 2D map is a function of the photoelectrode thickness which is shown by the SEM images in figure. Panels (c) and (d) are adapted from ref. [20] with permission from Elsevier, copyright 2017.

generation and recombination, is therefore an important parameter to take into account to control the 2D resolution. Two important parameters related to the diffusion length are the carrier lifetime τ and recombination rate R, related by $L = \sqrt{D\tau}$ and $\tau = n_{ph}/R$, where D is the diffusion coefficient and n_{ph} is the photogenerated minority carrier concentration. Direct band gap semiconductors, such as GaAs InAs and amorphous Si, are characterised by far faster recombination rates compared to indirect band gap semiconductors, such as Si and Ge (e.g. at a carrier concentration of 10^{18} cm^{-3} Si has a recombination rate of 10^{22} $s{\cdot}cm^{-3}$, compared to $5{\cdot}x\ 10^{26}$ $s{\cdot}cm^{-3}$ for GaAs). Precisely because of its short diffusion length – which is ironically regarded as a weakness in the field of photocatalysis and photovoltaics – thin layers of hydrogenated amorphous silicon (a-Si)[12, 21-23] are interesting for the goal of improving 2D resolution.

Moreover, increasing the doping level decreases τ (and therefore L) and indirect band gap semiconductor can also have high recombination rates if the level of defects is high enough. For example, hematite is highly promising indirect band gap candidate for 2D addressable electrochemistry.[13]

3.2 Electron transfer rate effects on 2D confinement

Besides the effect of diffusion lengths, charge transfer rates also affect the 2D resolution of a light-activated electrochemistry experiment. This was demonstrated by Erikson *et al.* while studying hydrogen evolution catalysed by adsorbed platinum.[24] Briefly, if the redox reaction rate is sufficiently high, minority carriers are consumed as soon as they are generated, hence limiting their lateral diffusion.

In a theoretical work, Scherson and co-workers have investigated the dependence of resolution on bias and light intensity.[25] They found that at high applied voltages, minority carriers are more likely to reach regions beyond the illuminated area. We have experimentally corroborated – yet not fully explained – this last point, i.e. a decrease in the spatial resolution for larger applied potentials.[26]

3.3 Backside versus topside illumination

We have shown an increase in spatial resolution by switching the illumination of the semiconductor from its backside ("dry side", Fig. 4a) to the topside ("wet side", Fig. 4b).[26] This is not

surprising as when using topside illumination photogenerated carriers are consumed by the electrochemical reaction as soon as generated, preventing them to diffuse away from the generation point (Fig. 4b). With backside illumination the carriers must cross a relatively long path until they reach the electroactive species (Fig. 4a).

However, despite its poorer 2D resolution, backside illumination is sometimes preferable, such as for the analysis light-sensitive species or when there is the requirement of a microscope or a camera hindering illumination from the electrolyte-side of the electrode. Moreover, the spatial resolution can be improved by thinning the photoelectrode. The resolution decreases with increasing the electrode thickness because the photogenerated carriers diffuse isotropically before reaching the space charge layer (Fig. 4a). For example, LAPS have shown that the resolution of silicon thin films of micrometre or less thickness on a transparent substrate using back-side illumination show a resolution comparable to top-side illumination.[4] Choudhury et al. have shown the relationship between substrate thickness and resolution by scanning electrochemical microscopy operating in surface generation/tip-collection mode (Fig. 4c).[20] A monolayer of ferrocene molecules on an n-type silicon electrode was oxidised by applying a positive potential under focused illumination, which in turn oxidises the ferricyanide present in solution. The illumination is by a light pointer from the 'dry' electrode face, and an SECM ultramicroelectrode tip, continuously scanning the solid/liquid interface, reduces the ferrocyanide generated at the surface and provides an image of the redox active spot. The size of redox active spot was shown to be inversely proportional to the semiconductor thickness (Fig. 4d). The redox process is imaged indirectly from the electrolyte 'point of view', and therefore SECM greatly overestimates the resolution for this light-addressable electrochemical reaction. That is, the size of the electroactive spot is probed with the additional complication of the mediator diffusing between the surface and the SECM tip, as the distance diffused, d, by a random walk after a time t depends on diffusivity, D, and is given by the relation $d=(2Dt)^{1/2}$.

4. Photoelectrode materials

The first decision to be taken in building a light-addressable electrochemical platform is the choice of the photoelectrode material. As a rule, the material should be compatible with the system (e.g. biocompatible, and bandgap matching the experimental conditions), unreactive towards the chemicals present in the electrolyte, and stable towards the light stimulus and applied bias. As discussed above (Section 3.1), it should also have a short carrier lifetime to ensure the electrochemical reaction is confined to the illuminated region. For some applications, transparency and flexibility are also required. In this section we review materials that have been used, or have the potential of being used, as photoelectrodes for light-addressable electrochemistry. Among them, although silicon is the most popular, quantum dots and photoconductive metal oxides, such as hematite, offer specific advantages.

4.1 Silicon

Silicon possesses unique characteristics that makes it an attractive candidate for light-addressable electrochemical platforms: (1) single crystal wafers are relatively inexpensive and readily available in a range of doping levels and types; (2) silicon is compatible with biological systems, such as cells;[9] (3) due to its narrow bandgap (1.1 eV) it can be excited using low energy visible light; (4) Si–C-bound organic monolayers are very stable and effective in preventing the oxidation of the silicon to silica under aqueous, oxygen-rich and anodic conditions. The organic monolayer tethered on the electrode is also a handle on its chemical properties. For example, the monolayer can be modified to bind selectively a specific analyte and this aspect has been exploited to prepare DNA arrays (*vide infra*, Section 6.1).[5] The monolayer can also serve for the attachment of chemically dynamic structures, such as a redox-responsive linker that was used to the release of specific single rare cells selected by a highly focused microscope light.[9]

Amorphous silicon (a-Si) is a disordered allotropic form of Si, and as such it shares most of the attractive characteristics discussed above. However, its short diffusion length, which remains its main drawback when used in a photovoltaic cell, makes it particularly attractive for a light-activated electrochemistry experiment (Section 3.1). Typical diffusion lengths for a-Si are in the order of few nanometres, in contrast with few micrometres for crystalline silicon, and the high spatial resolution for light-addressable electrochemistry on a-Si has been highlighted by Lim and by Suzurikawa.[23, 27]

Moreover, a-Si can be deposited as a thin-film layer on a conductive substrate. This is advantageous when using intrinsic (undoped) a-Si, because it behaves purely as a photoconductor. Charge transport in an intrinsic a-Si is not blocked in the dark by a highly resistive near-surface SCL, but in fact the whole depth of the undoped film is of extremely large resistivity. Charge carriers will only be generated up to a depth in the film where light can penetrate, and once generated, they will not travel far due to the a-Si short diffusion length. To transfer charges between a redox couple present in the electrolyte and the external circuit (e.g. the electrode back contact) the entire depth of the a-Si layer needs to be illuminated to maintain a "conductive channel" between the electrolyte and the electrical contact (Fig. 5a–b). The light penetration depth is dependent on the nature material and the light wavelength. For a-Si the penetration depth is ca. 4 μm for red light and ca. 1 μm for blue light. Therefore, the photoconductor needs to be thick enough to prevent appreciable current flowing under dark conditions by electron tunnelling, but at the same time thin enough to allow for light to penetrate its entire depth. Light-addressable electrochemistry on an intrinsic a-Si thin layer photoelectrode, and its dependence on wavelength, has been explored by us for the deposition of Cu_2O patterns.[10]

4.2 Quantum dots

Quantum dots are semiconducting nanoparticles with optical and electronic properties that can be tuned by modifying their composition, size and shape. Their band gap can be tuned

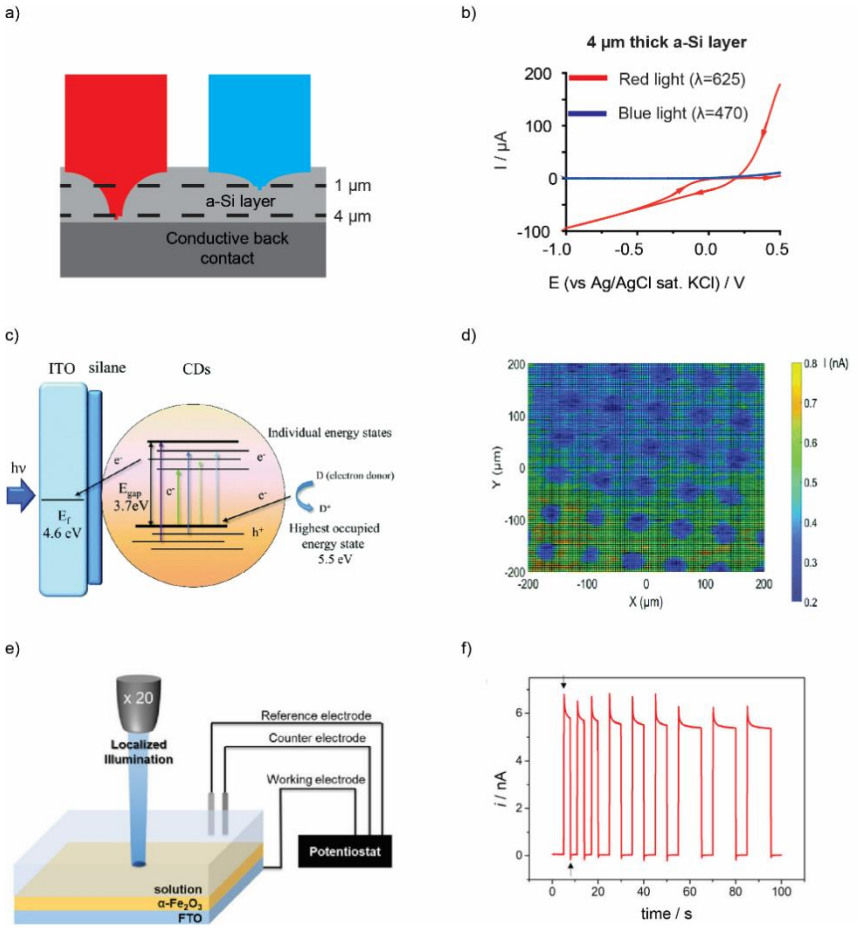

Fig. 5. Photoelectrode materials for light-addressable electrochemistry. a) Scheme of intrinsic a-Si photoelectrode representing the adsorption of two different wavelengths. b) Cyclic voltammograms for Cu_2O electrodeposition using two different light wavelengths for a 4 µm thick a-Si layer. c) Mechanism of photoelectric conversion of quantum dots (CDs). d) ac-photocurrent image of a PMMA dot array on the ITO-silane-CDs surface shown in c). e) Experimental scheme of hematite-based light-addressable electrochemistry. f) Photocurrent transient of ferrocyanide at a biased hematite photoelectrode using the experimental set-up shown in e). The arrows show when the light is turned on and off. Panels a) and b) are adapted from ref. [10] with permission from Wiley, copyright 2018; panels c) and d) are adapted from ref. [28] under the CC BY license;.and panels e) and f) are adapted from ref. [13] with permission from American Chemical Society, copyright 2018.

covering the whole UV-visible-IR range, they have very short diffusion lengths,[14] can be made from biocompatible materials stable under environmental conditions, and can be chemically modified. These features make quantum dots a promising material for photoelectrochemical detection.[14] Photoelectrochemical sensors based on quantum dots could be easily extended to perform spatially resolved electrochemical reactions, as suggested by Yue et al..[14] Krause and co-workers have recently shown the use of quantum dots as a photoelectrode for photoelectrochemical imaging (Fig. 5c–d).

4.3 Photoconductive metal oxides

Several metal oxides present photoconductivity, such as ZnO, TiO_2, Fe_2O_3 (hematite) and Al_2O_3, and are therefore suitable light-addressable photoelectrodes. These materials tend to form passive protecting layers, and their stability and breakdown leading to local dissolution and corrosion can be studied by photoelectrochemical microscopy.[8, 29-32] Light-addressable electrodeposition[7, 33-35] and light addressed water splitting[36] have been also demonstrated on metal oxide photoelectrodes.

Among the metal oxides, TiO_2, an n-type semiconductor with a bandgap in the UV range (ca. 3 eV), is of importance for historical reasons. It has played a central role in energy research since the discovery of water splitting by Honda and co-workers, and TiO_2 photoanodes have been used for light-addressable electrodeposition,[7, 33] light-addressed water splitting,[36] and photoelectrochemical microscopy.[8]

Hematite has a narrow bandgap (1.9–2.2 eV), is relatively stable, abundant, non-toxicity and has a short diffusion length (2–4 nm). A hematite thin film has been recently reported as a photoanode substrate for light-addressable electrochemistry (Fig. 5e) and shown capable of performing stable and reproducible amperometric analysis of dopamine (Fig. 5f). [13]

5. Surface patterning

One of the most successful applications to date of light-addressable electrochemistry is in the context of surface patterning: converting any arbitrary user-defined digital image into a metallic, polymeric or molecular pattern, by means of the combined effect of light and potential. This approach to create

patterns on an electrode surface can be fast (seconds or less), one-step and does not require physical masks, templates or inks. It is therefore an appealing alternative to established printing technologies, such as inkjet printers.[37] The light-assisted redox patterning can involve (i) direct electrodeposition, where the material being deposited is an electroactive species that is switched between soluble and insoluble depending on its redox state (e.g. a metal ion being discharged to its zero oxidation state, Fig. 6a), or (ii) an indirect deposition process, where an electrochemical reaction generates reactive chemical species that trigger a chemical change of the components present in the electrolytic solution (e.g. a chemical reaction induced by a redox-induced change in pH, Fig. 6b).

Notably, photoelectrochemical patterning has been the first successful example of light-addressable electrochemistry: first reported in 1978 by Honda and co-workers for metal and metal oxides patterning on TiO_2 and ZnO n-type electrodes.[7] In this early work soluble metallic ions were photoelectrochemically oxidised to an insoluble oxide form. Inspired by this work, several other groups during the 1980s reported on photoelectrochemical systems suitable to pattern the surface of metals and metal oxides.[33, 34] Noteworthy is the work of Yoneyama and Masahiro, and that of Honda and co-workers reporting the photoelectrochemical polymerization of pyrrole into polypyrrole patterns.[35, 38] Other polymers that have been patterned using light-addressable electrochemistry by direct electrodeposition are polythiophene[39] and polyaniline.[40]

5.1 Spatial light modulators for photoelectrochemical patterning

A travelling *x-y* stage offers a relatively simple set-up for patterning proof-of-principle works (Fig. 6c), but it has limitations. It imposes a sequential approach to the delivery of the light stimulus, which can be time consuming. A further complication is the risk of turning the areas covered by the pattern into an ohmic contact. This leads to patterns that continues to grow even in the dark. Because the sequential nature of the deposition when using a travelling stage, there is an increased chance for an area being patterned to continue growing when the light pointer has moved to the next section, resulting in a non-uniform and distorted pattern. In response to these shortcomings, several groups have moved towards the use of a microscale projector to control *at will* the time and shape of the illumination (e.g. possibility of parallel deposition), and fully exploiting the potential of photoelectrochemical patterning.[10, 21, 23, 41, 42]

We started research in this direction by developing a microprojector to draw patterns of Au and Cu$_2$O nanoparticles,[43] and have recently applied this to the assembly of Cu_2O nanocrystals with adjustable crystallographic structure and inter-particle spacing.[10] The microprojector set-up consists of a ferroelectric liquid crystal on silicon, operating as a spatial light modulator, coupled to a three-electrode electrochemical cell connected to a single-channel potentiostat (Fig. 7a–b). For example, Cu^{2+} ions are reduced to Cu^{+} under potentiostatic

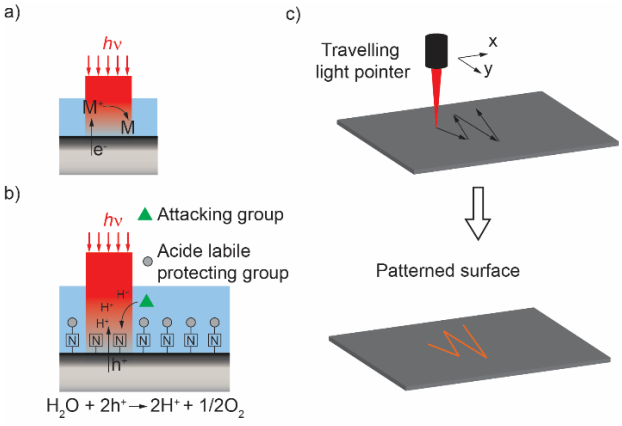

Fig. 6. Photoelectrochemical patterning. (a) Metal (M) photoelectrodeposition by reduction of a metallic ion (M+). (b) Indirect light-assisted electrodeposition by electrochemically generating protons (H^+) that attack an acid labile protecting group exposing a reactive functional group (N).[22] (c) Scheme of a travelling light-pointer set-up used for a photoelectrochemical deposition.

control to form the Cu_2O nanocrystals after hydrolysis (Fig. 7a). We found the spatial resolution to be a function not only of the illuminated area, but also of the amount of charge being transferred. As the transfer of charge progresses, the pattern grows laterally until reaching a saturation point, presumably because a large Cu_2O coverage reduces the efficiency of electron ejection, as suggested by conductive atomic force microscopy measurements.[10] By using a microprojector, inter-particle distances and nanocrystal morphology can be independently modulated by adjusting local light intensity, applied potential and chloride concentration (Fig. 7c).

We used the projector and adjustments of these three variable to build complex patterns over large areas (Fig 7d), and this has created a platform perfectly suited to investigate the electrical properties of single polyhedral nanocrystals,[11] and with the potential to open up a new anti-counterfeiting technology.[10]

Another example of using spatial light modulators for photoelectrochemical patterning has been reported by Li and co-workers.[44-46] In their approach, called by the authors "optically-induced electrodeposition" (OED), an AC voltage is applied between two electrodes. A 1 µm thick amorphous silicon (a-Si) layer is deposited on an ITO-coated glass slide act as the photoelectrode, and a liquid crystal device is used as the light projection system. Illumination of the a-Si is from its backside, allowing a CCD camera attached to a microscope to record, from the front side, the progress of the electrodeposition process. This set-up was used for the printing of Ag films[44, 45] and Au nanoparticles,[46] and applied for the construction of field effect transistors.[44] The reported spatial resolution was a remarkable 2.7 µm, and interestingly it is dependent on the AC voltage frequency and amplitude, with higher frequencies and amplitudes giving the best match between the illuminated area and the deposited pattern.
Chung and co-workers used a three-electrode electrochemical set-up and applied a pulsed DC potential for the patterning of Ni-Mo nanoparticles for its use as a catalyst for hydrogen production. Their set-up consisted on a digital micromirror

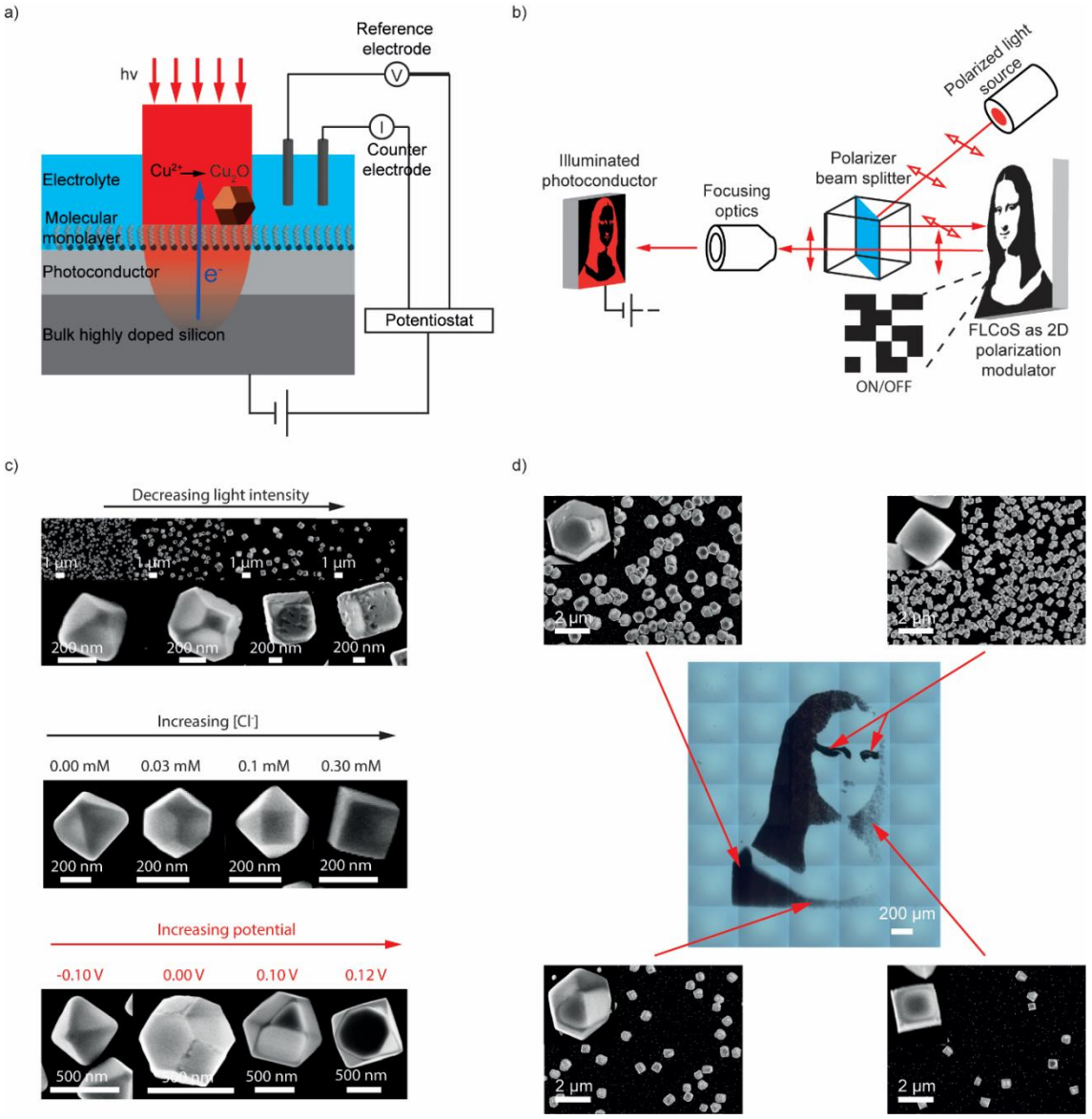

Fig. 7. Spatial light modulators for surface patterning. a) Scheme of the experimental set-up and working principle: Cu^{2+} ions in an electrolyte solution are photoelectrochemically discharged to Cu^{+} and hydrolysed to form Cu_2O nanocrystals on the electrode surface. Copper deposition is confined in space and time to illuminated regions of a photoconductor/electrolyte interface. The depiction of the interface, monolayer and particle is not to scale. (b) Scheme of the optical set-up: a user-defined image, or a sequence of images, is projected on the photoelectrode interface with this light pattern being defined by the ON/OFF status of each pixel of a ferroelectric spatial light modulator (schematically depicted as black and white squares in figure). This large array of ON/OFF ferroelectric liquid crystals elements (over 3 million of FLCoS pixels in the space of about 2 cm^2) changes (or not, *i.e.* empty arrows heads) the 2D pattern of the light polarization that it reflects back towards the electrode *via* a polarizer beam splitter, hence it defines the image projected on the electrified photoconductor. c) SEM images of Cu_2O nanoparticles and its progressively transition from cubic to octahedral shapes upon changes to either light intensity, bulk chloride, or deposition potential. d) Gradients of shapes and densities embedded in a "Mona Lisa" pattern. Adapted from ref. [10] with permission from Wiley, copyright 2018 and ref. [11] with permission from American Chemical Society, copyright 2018.

device providing topside illumination of an a-Si thin layer with a p-i-n (p-type, intrinsic, n-type) structure deposited on a monocrystalline silicon wafer as the photoelectrode.[23]

5.2 Photoelectrochemical patterning of non-redox species

Although all the examples given above relates to the patterning of electroactive species, the concept of photoelectrochemical patterning is not limited to redox systems. It has been shown that light-addressable electrochemistry can be used for the deposition of non-electroactive species. For example, the photoelectrochemical generation of chemical gradients, or redox-induced changes to pH, can guide the deposition of polymers, hydrogels, or the attachment of molecules onto solid surfaces. Research on this theme was first reported in 2009 by Jacobson and co-workers,[22] showing that photoelectrochemically produced protons induce the cleavage of an acid labile protecting group assembled on a surface. Deprotected molecules react with reagents in solution to form covalent bonds (Fig. 6b), and the synthesis of a DNA microarray

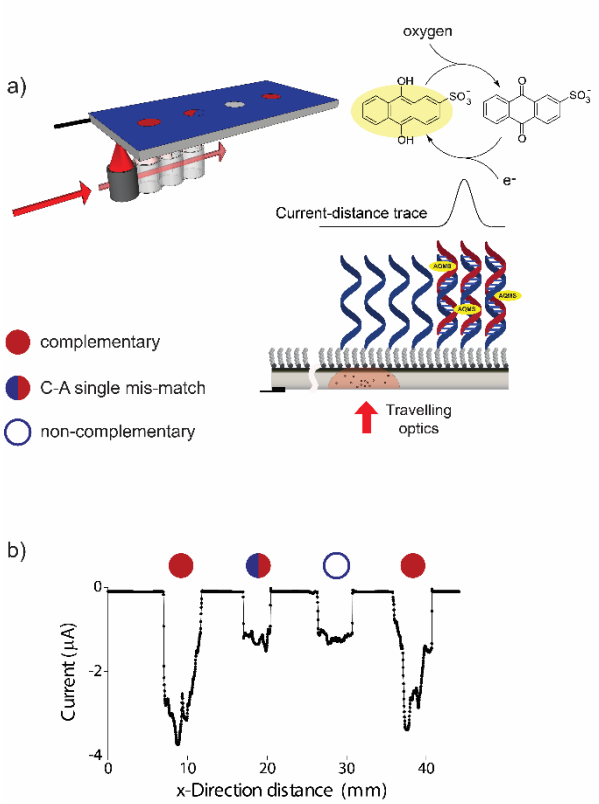

Fig. 8. Demonstration of "electrochemical reading" from a DNA array. a) Schematics of a modified silicon photocathode device capable of spatially resolving DNA hybridization. b) Electrochemical response, linked to DNA hybridisation events, as function of the position of a light source that travels across the length of a single-wire, four element, DNA array on Si(100) electrodes. Reproduced from ref. [5] under the CC BY license.

platform was used to highlight some of the merits of this approach. Huang *et al*. have demonstrated the synthesis of calcium alginate hydrogels patterns triggered by photoelectrochemically produced protons; protons dissolve dispersed $CaCO_3$ and the Ca^{2+} being released led to the crosslinking of alginate present in the electrolytic solution.[47] The authors also demonstrated the encapsulation of cells in these alginate hydrogel patterns[47] and the encapsulation of enzymes entrapped in chitosan.[42] For the case of chitosan, a change in pH makes it insoluble and induces its crosslinking. Other example of light-addressable electrochemistry for the printing of non-electroactive species include the polymerization of acrylate-based molecules initiated by hydrogen radicals generated from the photoelectroreduction of protons.[48] This approach, developed by Li and co-workers, was used to synthesize multi-layered and 3D structures with a spatial resolution of just few microns.[21, 41]

6. Multielectrode arrays without leads

Since the development of integrated circuit fabrication technologies in the 1970s, individually addressable microelectrode arrays have become a powerful tool in electrochemical analysis, offering high spatial resolution and being both sensitive and specific.[1] An intrinsic feature of an electrode array is the requirement of each independent electrode to be wired to an external circuit. This requires considerable space that limits the electrode density in an array, and the array geometry is predefined and cannot be adjusted during the experiment. Light-driven sensors that offer a clean and adaptable stimulus are of special interest. A most notable example is the light addressable potentiometric sensor (LAPS).[4]

LAPS belong to the electrolyte/insulator/silicon field effect sensor family and consist of a low doped semiconductor with an insulating layer in contact with the electrolyte. A potential is applied between the silicon and the solution and an AC photocurrent is generated in response to a rapidly modulated light source. Surface chemical changes can be inferred from the photo-response. By directing the light beam to a specific location of the surface it is possible to obtain local information on the charging of the interface, and used for example as a surface activity imaging tool. Because the presence of an insulating layer at the interface, LAPS do not allow to alter the net rate of a heterogeneous electrochemical reaction, hence it remains a potentiometric sensing device. This last point marks the principal difference between LAPS and the concept of light-addressable electrochemistry, where a net photoelectrochemical reaction takes place and an amperometric measurement is possible. Nonetheless, LAPS have been proven to be a powerful tool for chemical and biochemical imaging and sensing. Much of the knowledge acquired and methodologies used by LAPS provide a good starting point for light-addressable electrochemistry, as both rely on photoeffects at the semiconductor/liquid interface. For example, as we have seen in Section 3, their equivalences regarding spatial resolution are evident. Higher resolutions are obtained when using photoelectrodes with fast recombination rates and front side illumination (or back side illumination and a thin photoconductor layer). It is also of interest for light-addressable electrochemistry the experimental set-ups used for LAPS. A good example of this is the flexibility that projection system offers to modulate the light.[4]

Also relevant is the field of photoelectrochemical sensors.[14] Photoelectrochemical sensors generate photocurrents that are sensitive to the chemical environment. The immediate implication is that the principle of photoelectrochemical sensing can be easily extended to light-addressable electrochemical sensors by spatially confining the illumination in 2D. This principle allows to spatially resolve the sensing of elements akin to multielectrode arrays.[5] This section introduces and reviews the principles of light-addressable electrochemical sensors.

6.1 Light-addressable electrochemistry as an amperometric sensor

The use of light-addressable electrochemistry for chemical sensing was opened in 2015 through the work of Choudhury *et al*.[5] In this proof-of-principle work, Choudhury *et al.* used silicon as the semiconductor substrate. The small bandgap of silicon

(1.1. eV) is such that visible light can be used, which becomes important for biological applications. At the same time, silicon's surface reactivity towards unsaturated carbon–carbon bonds makes it a suitable platform for achieving specific surface functionalities. Choudhury *et al*. chemically modified a low-doped silicon electrode with an α,ω-dialkyne molecule which passivates the surface but also provides a chemical path for the attachment of an array of DNA probes (Fig. 8a). A single-stand DNA analyte was added to the electrolyte, and whether DNA duplexes were formed at each spot in the array was determined electrochemically by scanning the light source across the array. This DNA detection scheme requires the presence of a redox-active intercalator in solution, such that an enhanced current is observed when the light passes over a spot containing duplexes (Fig. 8b).

Considering the early stage of the field, there is still much to learn on the experimental parameters effecting analyte detection. In addition to variables to be considered in a conventional electrochemical sensing system, there are some specific to light-addressable electrochemistry. Among them are the role of light intensity, wavelength, semiconductor doping type and level, substrate thickness, substrate diffusion length and illumination side (i.e. topside *vs* backside). Since Choudhury *et al.* work, a few reports have started a systematic study of some of these parameters. For example, Seo *et al.* have performed a quantitative analysis for the detection of dopamine.[13] They used hematite as a photoanode and a 5 μm laser spot shining from the electrolyte side. They studied how the illuminated area and the light intensity affect the photocurrent and their effect on the sensor calibration curve. A stronger light intensity or a larger illuminated area rises the photocurrent leading to a higher sensitivity. The total exposed electrode area to the electrolyte solution affects the detection limit, with a smaller exposed area reducing the signal noise therefore increasing the detection limit.

7. Photoelectrochemical microscopy

As introduced in Section 1, over the last 30 years, several developments in the fields of catalysis, energy and sensing have been possible thanks to scanning electrochemical probe microscopy (SEPM) techniques.[2] In these redox imaging techniques a microelectrode is scanned over the substrate and the local electrochemical activity is studied from the electrolyte perspective. The tip-to-substrate distance is not maintained constant throughout the scanning (Fig. 9a)[2] and it is often hard to deconvolute morphology from electroactivity. The generation of convective forces by the scanning tip needs to be avoided, especially for high viscosity electrolytes and species with low diffusion coefficient.

As we have covered in this Tutorial, using a photoconductor surface the electrochemical reaction can be confined at a certain area by local illumination. The photocurrent is linked to the local surface activity, and by scanning the light spot over the entire surface (Fig. 9b), several current readings can be used to generate a photocurrent image. Photoelectrochemical microscopy, in contrast with SEPM, investigates the electrochemical process from the surface perspective, i.e. a certain area of a photoconductor electrode is transiently 'activated' by localizing a light spot and the generated photocurrent is immediately collected from a single lead connected to the electrode itself (Fig. 9b). The current magnitude depends on the local activity of the interface because of changes in composition or catalytic centres. For example, in Fig. 9b ferrocene molecules patterned on a photoanode provides a catalytic 'line' for the oxidation of a redox species in solution: a line-shaped spike in current is

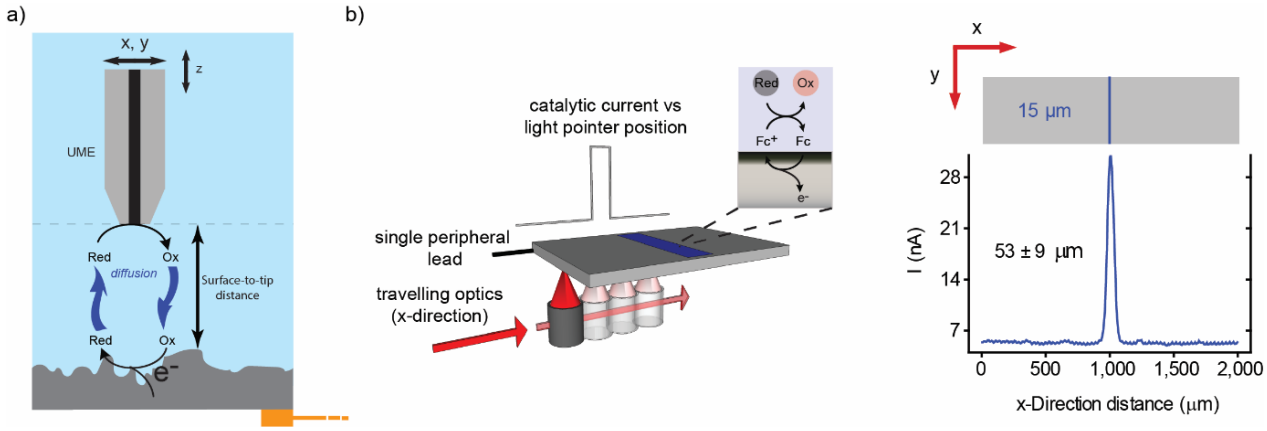

Fig. 9. Electrochemical microscopy. (a) Scheme of the general working principle of a standard scanning electrochemical probe technique. (b) Light-addressable electrochemical imaging of a discrete redox feature and an example of the experimental output (catalytic current vs light pointer position). A travelling light bean moves along the x-direction to illuminate the back-side of a macroscopic n-type silicon electrode. On the upper side, in contact with an electrolytic solution containing a diffusive redox couple, is a "line" of surface-bound ferrocene molecule. The width of the line (15 μm) is known. The faradaic current based on the heterogeneous charge transfer, i.e. a catalytic current–time trace, is recorded as a function of the light pointer travelling distance. The device can afford a two-dimensional electrochemical information through a single distal wire; i.e., resolving the width of an electroactive "line" feature. Part b) is adapted from reference [5] under the CC BY license.

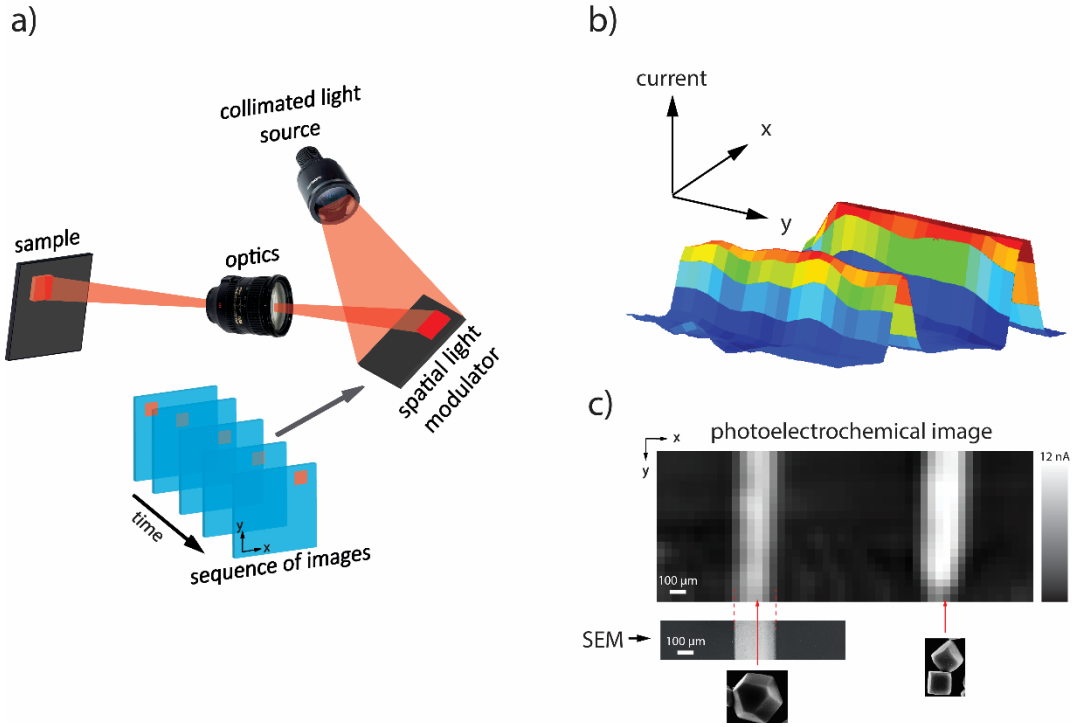

Fig. 10. Electrochemical microscopy based on spatial light modulators. a) Simplified scheme of the working principle of a "projector" based on spatial light modulators. A user-defined image, or a sequence of images, is projected on an electrified interface, with the light pattern being defined by the ON/OFF status of each pixel of the spatial light modulator. b) Current–time data aquired on a silicon photoanode modified with two parallel "lines" of Cu_2O nanoparticles catalysing the electro-oxidation of methanol. Each scan along the sample's x-axis takes 5.9 s, with a total of 10 scans (along the y-axis) plotted. c) 2D map (electrochemical image) constructed from current-time data that are linked to a specific x-y coordinate. The redox map is a match of the SEM image (lower panels) and reveals a higher metanol electro-oxidation activity for cubic Cu_2O nanoparticles. Part a) and c) are adapted from reference [12] under the CC BY license.

observed as the light pointer moves across the ferrocene feature (Fig. 9b, right panel).

The concept of photoelectrochemical microscopy was introduced by Butler in the early 1980s[8] and was further developed by Williams,[29] Atanasoski [30] and Bicelli[31] for the study of corrosion processes on metal electrodes. Since the passivating layer formed on some metal electrodes can behave as a photoelectrode it is possible to obtain local photoelectrochemical information by local illumination. Williams and co-workers have also investigated the effects on the form of the image depending on the light intensity, beam size, potential and scan speed and developed a theoretical model to explain the results.[32] More recently, with the advent of stable photoelectrodes, photoelectrochemical microscopy is showing its potential prospects for bioanalytical imaging.[28] and photocatalysts screening.[12, 49]

7.1 Photoelectrochemical microscopy based on spatial light modulators

We have explored the possibility of photoelectrochemical microscopy by using a spatial light modulator to project in rapid sequence images of a single bright "pixel" (Fig. 10a) while recording the current of the electrochemical reaction.[12] The current–time signal is linked to the temporal sequence and x-y coordinates of each illumination event, and this generates a redox map of the electrode surface (Fig. 10b–c). In this way 2D electrochemical information is acquired without resorting to physically moving parts. The use of a spatial light modulator instead of a travelling light pointer allows for greater experimental freedom; the illuminated area, geometry, sequence, light intensity or scanning frequency are completely customizable. In our first proof-of-principle example we interrogated an amorphous silicon substrate patterned with cuprous oxide particles acting as catalytic sites for both electro-reduction and electro-oxidation heterogeneous reactions (Fig. 10c). As depicted in Fig. 10a, while applying a constant potential to the amorphous silicon substrate, over one thousand individual images of discrete light squares of 46x46 µm are projected on the electrode in rapid sequence at a frequency of 17 Hz. Each projected square corresponds to a specific x-y coordinate and a specific time, which makes it possible to link to the recorded electrochemical current–time signal to a location on the electrode surface. Electrochemical images were recorded at a rate of ca. one frame per minute (1000 projected images and 59 ms dwell time per image) and the 2D redox map does accurately match the geometry of the surface features (Fig. 10c, 2D distribution of the surface activity towards methanol oxidation). Using the "write" mode of the spatial light modulator we prepared a two line-shaped arrays of nanoparticles of different shapes, and have been able to show that cubic particles present a higher activity than polyhedral particles (Fig. 10c) toward this model electro-oxidation reaction. This result is significant, as electron ejection from Cu_2O particles is known to be relatively less pronounced in cubic over polyhedral Cu_2O nanocrystals,[11] therefore suggesting that more factors are involved in the electrochemical oxidation (e.g.

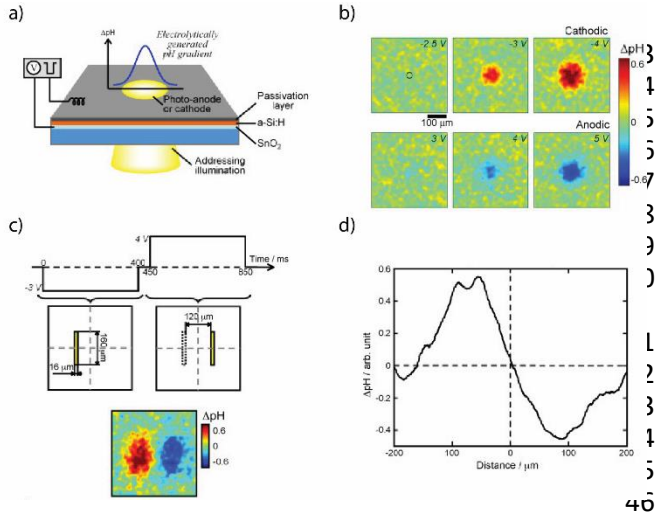

Fig. 11. Generation of a pH gradient by light-addressable electrolysis. a) Schematic diagram of pH gradient generation by light-addressable electrochemistry. b) Fluorescence images of generated pH gradients by light-addressed anodic and cathodic electrolysis. c) Fluorescence image of the superposition of two pH gradients. d) Time-potential-light pattern projected sequence (above) and cross-section profile of the pH pattern shown in c (below). Adapted from ref. [27] with permission from Elsevier, copyright 2010.

facet dependent chemical adsorption) over an exclusive electrical process. It is important to stress that when trying to compare the catalytic activity of different materials (in this case Cu cubes nanocubes versus Cu_2O polyhedrons), having them subject to exactly the same experimental conditions (same substrate, illumination and electrolyte) removes a great deal of experimental ambiguity. This electrochemical microscopy technique is in principle applicable to any semiconductor under depletion or any photoconductor. We also demonstrated the use of this technique for electro-reduction reactions, more specifically for the carbon dioxide photoreduction.[12] This demonstrates the use of spatial light modulators and light-addressable electrochemistry as a powerful tool for electrochemical imaging, especially for the highly parallel screening of the catalytic activity of an array of catalysts. [12, 49]

8. Generation of chemical gradients

Chemical gradients play an important role in biological systems and processes. Gradient generation methods are gaining popularity for the study of these biological mechanisms and the engineering of bioinspired energy production machines, moving droplets and molecular motion.[50] There are many gradient generation methods; most notably examples are microfluidic devices and electrochemical methods.[50] For practical purposes these gradients need to be flexible enough to represent different experimental situations. Light-addressed electrochemical reactions offer the possibility of creating flexible and dynamic gradients in space and time on an unstructured surface.[27, 36] Suzurikawa et al. first demonstrated this possibility by generating pH micro-gradients using a digital micromirror device and an a-Si photoelectrode (Fig. 11a).[27] Protons and hydroxide anions were locally generated by the light-addressed chlorine hydrolysis and reduction of water, respectively (Fig. 11a). The formed gradients were imaged by fluorescence microscopy in the presence of a fluorescent pH indicator (Fig. 11b). The digital micromirror device allows the projection of light patterns that can be converted into pH gradient patterns, with a resolution of few micrometers. The dynamic interplay of polarization and light allows for the superposition of pH gradients (Fig. 11c and d).

9. Outlook

In summary, established concepts of photovoltaics, photocatalysis and solid-state semiconductor physics are merged using surface chemistry as the common element and used to create a simple approach to confine electrochemical reactivity in 2D. Using light as a 'clean' stimulus to activate transient conductive channels across a monolithic and unstructured semiconductor electrode lifts limitation imposed by physical probes or arrays of electrodes. For example, by using commercially available spatial light modulator it is possible to individually address over 3 million discrete regions of a substrate 1 × 1 cm in size; without the need of individual electrical leads, multi-channel instruments, or moving parts. It gives a greater freedom and complements traditional methods such as scanning electrochemical probes or multielectrode arrays.

Although still in its infancy, this field appears promising for the development of a host of applications. We have discussed the proof-of concept experiments in micropatterning, chemical analysis, redox microscopy and generation of chemical gradients. Photoelectrochemical patterning offers an alternative to traditional methods for creating microstructures on semiconductor substrates. It is a non-sequential, fast and economic method. It avoids the common coffee ring effect characteristic from inkjet printers, and in contrast to photolithography, it does not require multiple steps, aggressive chemicals or UV radiation.

Light-addressable electrochemistry is a tool for electrochemical analysis, akin to multielectrode arrays, but without geometrical restrictions and requiring a single electrical lead. When usedas a redox imaging instrument it extends and complements the information that one obtains by scanning probe techniques. Other application are opening up for light-addressable electrochemistry, and of special interest is its impact in cell biology research. In a recent report we have used it as a platform for the isolation of rare single cells.[9] We have captured cells on an unstructured surface that was modified with an organic monolayer presenting antibodies targeting specific cell antigens. A quinone trimethyl lock system that undergoes reductive lactonisation (ring closure) served as a redox "switchable" component embedded in the monolayer. This cleavable linker releases the antibody at the distal end of the monolayer when reduced (Fig. 12a) and a light pointer localises this redox reaction to a selected region of the surface, allowing for the release of single cells (Fig. 12b). This cell biology work builds upon all of the key features of light-addressable

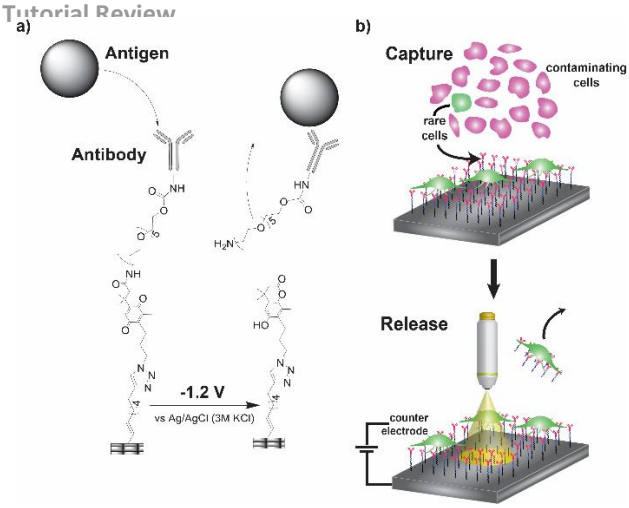

Fig. 12. Photoelectrochemical release of single rare cells. a) The antigen present in the rare cells binds specifically with the antibody tetheret to a silicon surface via a switchable component consisting on a trimethyl lock system. The switchable component when a reduction potential is applied undergoes lactonization and is cleaved, releasing the cells. b) Schematics of the capture and release platform. The release of single cells is possible by localizing the light beam on a single cell while applying a reduction potential. Adapted from ref. [9] under the CC-BY license.

electrochemistry, in that there is no pre-organised surface architecture, total freedom in geometry of the activated region and only one connecting lead. This platform could be used to select cells based on their response to drugs and other stimuli, morphology or surface expression.

Conflicts of interest

There are no conflicts to declare.

Acknowledgements

The work presented herein was supported by funding from the Australian Research Council (DP1094564, CE140100036, DP150103065, FL150100060, DE160100732, DP190100739) and from the National Health and Medical Research Council (1091261).

Notes and references

1. C. N. LaFratta and D. R. Walt, *Chem. Rev.*, 2008, **108**, 614-637.
2. D. Polcari, P. Dauphin-Ducharme and J. Mauzeroll, *Chem. Rev.*, 2016, **116**, 13234-13278.
3. X. Shan, U. Patel, S. Wang, R. Iglesias and N. Tao, *Science*, 2010, **327**, 1363-1366.
4. F. Wu, I. Campos, D.-W. Zhang and S. Krause, *Proc. R. Soc. A*, 2017, **473**, 20170130.
5. M. H. Choudhury, S. Ciampi, Y. Yang, R. Tavallaie, Y. Zhu, L. Zarei, V. R. Goncales and J. J. Gooding, *Chem. Sci.*, 2015, **6**, 6769-6776.
6. H. O. Finklea, *Semiconductor Electrodes*, Elsevier, Amsterdam, 1988.
7. T. Inoue, A. Fujishima and K. Honda, *Chem. Lett.*, 1978, **7**, 1191-1200.
8. M. A. Butler, *J. Electrochem. Soc.*, 1983, **130**, 2358-2362.
9. S. G. Parker, Y. Yang, S. Ciampi, B. Gupta, K. Kimpton, F. M. Mansfeld, M. Kavallaris, K. Gaus and J. J. Gooding, *Nat. Commun.*, 2018, **9**, 2288.
10. Y. B. Vogel, V. R. Gonçales, L. Al-Obaidi, J. J. Gooding, N. Darwish and S. Ciampi, *Adv. Funct. Mater.*, 2018, **28**, 1804791.
11. Y. B. Vogel, J. Zhang, N. Darwish and S. Ciampi, *ACS Nano*, 2018, **12**, 8071-8080.
12. Y. B. Vogel, V. R. Gonçales, J. J. Gooding and S. Ciampi, *J. Electrochem. Soc.*, 2018, **165**, H3085-H3092.
13. D. Seo, S. Y. Lim, J. Lee, J. Yun and T. D. Chung, *ACS Appl. Mater. Interfaces*, 2018, **10**, 33662-33668.
14. Z. Yue, F. Lisdat, W. J. Parak, S. G. Hickey, L. Tu, N. Sabir, D. Dorfs and N. C. Bigall, *ACS Appl. Mater. Interfaces*, 2013, **5**, 2800-2814.
15. A. Fujishima and K. Honda, *Nature*, 1972, **238**, 37.
16. Y. B. Vogel, A. Molina, J. Gonzalez and S. Ciampi, *Anal. Chem.*, 2019, **91**, 5929-5937.
17. N. S. Lewis, *Inorg. Chem.*, 2005, **44**, 6900-6911.
18. Y. B. Vogel, L. Zhang, N. Darwish, V. R. Gonçales, A. Le Brun, J. J. Gooding, A. Molina, G. G. Wallace, M. L. Coote, J. Gonzalez and S. Ciampi, *Nat. Commun.*, 2017, **8**, 2066.
19. L. Zhang, Y. B. Vogel, B. B. Noble, V. R. Gonçales, N. Darwish, A. L. Brun, J. J. Gooding, G. G. Wallace, M. L. Coote and S. Ciampi, *J. Am. Chem. Soc.*, 2016, **138**, 9611-9619.
20. M. H. Choudhury, S. Ciampi, X. Lu, M. B. Kashi, C. Zhao and J. J. Gooding, *Electrochim. Acta*, 2017, **242**, 240–246.
21. Y. Li, S. Lai, N. Liu, G. Zhang, L. Liu, G.-B. Lee and W. Li, *Micromachines*, 2016, **7**, 65.
22. B. Y. Chow, C. J. Emig and J. M. Jacobson, *Proc. Natl. Acad. Sci. U. S. A.*, 2009, **106**, 15219.
23. S. Y. Lim, Y.-R. Kim, K. Ha, J.-K. Lee, J. G. Lee, W. Jang, J.-Y. Lee, J. H. Bae and T. D. Chung, *Energy Environ. Sci.*, 2015, **8**, 3654-3662.
24. S. Eriksson, P. Carlsson, B. Holmström and K. Uosaki, *J. Appl. Phys.*, 1991, **69**, 2324-2327.
25. H. Zhu, B. Miller and D. Scherson, *J. Electrochem. Soc.*, 2010, **157**, F137-F143.
26. Y. Yang, S. Ciampi, Y. Zhu and J. J. Gooding, *J. Phys. Chem. C*, 2016, **120**, 13032-13038.
27. J. Suzurikawa, M. Nakao, R. Kanzaki and H. Takahashi, *Sens. Actuators, B*, 2010, **149**, 205-211.
28. D.-W. Zhang, N. Papaioannou, N. M. David, H. Luo, H. Gao, L. C. Tanase, T. Degousée, P. Samorì, A. Sapelkin, O. Fenwick, M.-M. Titirici and S. Krause, *Mater. Horiz.*, 2018, **5**, 423-428.
29. A. R. J. Kucernak, R. Peat and D. E. Williams, *Electrochim. Acta*, 1993, **38**, 71-87.
30. P. S. Tyler, M. R. Kozlowski, W. H. Smyrl and R. T. Atanasoski, *J. Electroanal. Chem. Interfacial Electrochem.*, 1987, **237**, 295-302.
31. S. Maffi, C. Lenardi, B. Bozzini and L. P. Bicelli, *Meas. Sci. Technol.*, 2002, **13**, 1398.
32. A. R. Kucernak, R. Peat and D. E. Williams, *J. Electrochem. Soc.*, 1991, **138**, 1645-1653.
33. T. Inoue, A. Fujishima and K. Honda, *J. Electrochem. Soc.*, 1980, **127**, 1582-1588.
34. T. L. Rose, R. H. Micheels, D. H. Longendorfer and R. David Rauh, *MRS Proceedings*, 1982, **17**, 265.
35. M. Okano, K. Itoh, A. Fujishima and K. Honda, *J. Electrochem. Soc.*, 1987, **134**, 837-841.
36. H. M. Maltanava, S. K. Poznyak, D. V. Andreeva, M. C. Quevedo, A. C. Bastos, J. Tedim, M. G. S. Ferreira and E. V. Skorb, *ACS Appl. Mater. Interfaces*, 2017, **9**, 24282-24289.
37. P. Calvert, *Chem. Mater.*, 2001, **13**, 3299-3305.
38. H. Yoneyama and K. Masahiro, *Chem. Lett.*, 1986, **15**, 657-660.

39. H. Yoneyama, K. Kawai and S. Kuwabata, *J. Electrochem. Soc.*, 1988, **135**, 1699-1702.
40. C. Janáky, N. R. de Tacconi, W. Chanmanee and K. Rajeshwar, *J. Phys. Chem. C*, 2012, **116**, 19145-19155.
41. P. Li, H. Yu, N. Liu, F. Wang, G.-B. Lee, Y. Wang, L. Liu and W. J. Li, *Biomater. Sci.*, 2018, **6**, 1371-1378.
42. S.-H. Huang, L.-S. Wei, H.-T. Chu and Y.-L. Jiang, *Sensors*, 2013, **13**, 10711-10724.
43. Y. B. Vogel, N. Darwish, M. B. Kashi, J. J. Gooding and S. Ciampi, *Electrochim. Acta*, 2017, **247**, 200-206.
44. N. Liu, F. Wei, L. Liu, H. S. S. Lai, H. Yu, Y. Wang, G.-B. Lee and W. J. Li, *Opt. Mater. Express*, 2015, **5**, 838-848.
45. P. Li, N. Liu, H. Yu, F. Wang, L. Liu, G.-B. Lee, Y. Wang and W. J. Li, *Sci. Rep.*, 2016, **6**, 28035.
46. N. Liu, M. Li, L. Liu, Y. Yang, J. Mai, H. Pu, Y. Sun and W. J. Li, *J. Micromech. Microeng.*, 2018, **28**, 025011.
47. S.-H. Huang, H.-T. Chu, Y.-M. Liou and K.-S. Huang, *Micromachines*, 2014, **5**, 1173.
48. N. Liu, P. Li, L. Liu, H. Yu, Y. Wang, G. Lee and W. J. Li, *J. Microelectromech. Syst.*, 2015, **24**, 2128-2135.
49. P. S. Shinde, X. Peng, J. Wang, Y. Ma, L. E. McNamara, N. I. Hammer, A. Gupta and S. Pan, *ACS Appl. Energy Mater.*, 2018, **1**, 2283-2294.
50. S. O. Krabbenborg and J. Huskens, *Angew. Chem. Int. Ed.*, 2014, **53**, 9152-9167.

Table of contents entry graphics.
Light-addressable electrochemistry: one wire, many electrodes